

## **ABSTRACT**

The data that is currently being loaded in near real-time into the database of the Hurricane Research Division's (HRD) H\*Wind wind analysis system, representing the measurements made by the SeaWinds instrument aboard NASA's QuikSCAT satellite, uses Aviation Model (AVN) circulation centers for determining wind direction solutions in the vicinity of TCs. The current dealiasing method used to process the QuikSCAT data incorporates the AVN model circulation centers, which can be up to six hours old by the time the data is collected, and may not even depict a circulation center in the model. Using aircraft reconnaissance fixes to locate the center of the TC at the time of the QuikSCAT observations, the wind vectors can be dealiased by finding the assumed flow around the TC and the radius of the effect of the storm on its surroundings. This method will provide the user with a more reasonable representation of the QuikSCAT winds for performing a surface wind analysis.

## **1. INTRODUCTION**

The Hurricane Research Division (HRD) developed a real-time objective wind analysis system (H\*Wind) (Powell et al. 1998, Otero et al. 2000) to document landfall episodes and assist hurricane and storm surge specialists at the National Hurricane Center (NHC) with their operational forecasts. H\*Wind provides the user with an interactive, graphical quality control tool for assessing various observation platforms (reconnaissance aircraft, GPS dropsondes, buoys, ships, wind measuring satellites, etc.) that are available for a given time period. Measurements

from NASA's SeaWinds instrument aboard the QuikSCAT are provided to H\*Wind by NOAA/NESDIS.

SeaWinds uses a single 1 meter parabolic antenna dish with two conically scanning spot beams to transmit radiation at 13.4 GHz toward the sea surface, which is then scattered back towards the emitting antenna (Katsaros et al. 2001). Changes in local wind stress cause changes in ocean surface roughness, which, in turn, modifies the radar cross-section of the body of water and the magnitude of the backscattered power. The mechanism responsible for scattering the energy is caused by selective interference from different elements on the surface. (Ulaby et al. 1986). The intensity of the backscattered radiation is proportional to the amplitude of the capillary waves, spawned by local wind stress, that propagate along the larger swell waves. Bragg resonant scattering provides the ocean wavelengths,  $L_i$ , that allow for significant backscatter to be received by the antenna. Ocean wavelengths that satisfy the Bragg scattering condition that for an incoming electromagnetic wave of wavelength,  $\lambda$ , at an angle of incidence,  $\theta$ :

$$(2L/\lambda) * \sin \theta = n \quad (1)$$

for

$$n = 0, 1, 2, \dots$$

are picked up by the radar.

The sun-synchronous instrument has a continuous swath measuring 1800 km, and provides 25-km resolution as it orbits the Earth 14.25 times a day at an altitude of 803 km above the surface at the equator. SeaWinds covers approximately 90% of the Earth every day, and is capable of measuring surface winds under all weather and cloud conditions over the ocean because atmospheric motions themselves do not considerably affect the radiation emitted and

received by the radar (Lungu 2001), thus proving to be a valuable instrument to oceanographers, climatologists and atmospheric scientists.

Currently, the QuikSCAT surface wind measurements brought into H\*Wind are processed by NESDIS, using Aviation Model (AVN) forecast runs to determine a first guess of the surface wind direction field. The problem with using the first guess values is that the model forecast can include initialized data that is up to six hours old before the QuikSCAT data is collected. This time lag can result in incorrectly-placed or poorly-defined circulation centers. In this paper, data sets from QuikSCAT passes for 2001 Hurricanes Iris (8 October) and Michelle (4 November and 5 November) containing the four initial wind ambiguities and the NESDIS first guess solution, were analyzed to justify the supposition that an algorithm using aircraft reconnaissance fixes to choose the best wind solutions within a TC will provide a more reasonable representation of the TC surface wind field. This paper gives insight into how the dealiasing algorithm is developed, as well as how it fares when tested on the above data sets.

## **2. METHODOLOGY**

An algorithm is desired that evaluates all available wind ambiguity solutions, within the radius of the TC's influence, relative to a given 'TC guess' that is based upon the center of circulation provided by aircraft reconnaissance fixes.

### *a. NESDIS processing and 'TC guess' wind direction*

The near real-time data received into H\*Wind will contain all four wind ambiguities and the one vector designated by NESDIS based upon Aviation Model (AVN) runs, which may not be at the time of the QuikSCAT pass. The center position chosen by the user in H\*Wind will serve

as the focal point of all observations, reflecting more recent, operational vortex centers in determining the assumed flow direction, or ‘TC guess’ solution. The azimuth relative to north,  $\alpha$ , for each observation location is calculated by:

$$\alpha = 90^\circ - \tan^{-1}(\lambda_v/\phi_v), \quad (2)$$

with

$$\lambda_v = (\lambda_o - \lambda_c) * 111.11 \text{ km} \quad (3)$$

and

$$\phi_v = (\phi_o - \phi_c) * \cos[(\lambda_o + \lambda_c)/2] * 111.11 \text{ km} \quad (4)$$

The virtual latitude,  $\phi_v$ , and virtual longitude,  $\lambda_v$ , in kilometers, represent the location of the observation recorded by SeaWinds (latitude,  $\phi_o$ , and longitude,  $\lambda_o$ ), relative to the center latitude and longitude,  $\phi_c$  and  $\lambda_c$ , respectively. This value is used to calculate the tangential wind,  $v_t$  at that point. From that tangential wind direction, an inflow angle will be subtracted, representing the inward directed flow toward the circulation center of the TC. The resulting flow is considered in determining the ‘TC guess’ solutions. Once that flow has been calculated, each of the four wind ambiguities for a given location can be compared to the ‘TC guess’ solution

#### *b. Surface wind inflow*

In 1996 the National Center for Atmospheric Research (NCAR) completed the development of the Airborne Vertical Atmospheric Profiling System (AVAPS), the Global Positioning System (GPS) dropwindsonde system used in NOAA and Air Force aircraft reconnaissance missions (Hock and Franklin 1999). These dropsondes are capable of transmitting location, pressure, temperature, humidity, and vertical wind profilers back to workstations aboard the aircraft. Because the vertical resolution is approximately 5 m, these

dropsondes can measure near-surface (10m) winds with accuracies of 0.5-2.0 m s<sup>-1</sup>. Over seventy-five NOAA GPS dropsondes that had reached the surface in Hurricane Keith (2000), Hurricane Gabrielle (2001), Hurricane Humberto (2001), and Hurricane Michelle (2001) were analyzed to find an observed average surface inflow. The center of the storm at the time of each dropsonde was represented by the interpolated location between aircraft reconnaissance fixes of the circulation center. To eliminate the measurements inside of the eye where there is no significant cyclonic rotation as well as those far away from the center, the inflow angle was averaged among sondes greater than 10 km from the center and less than 550 km away. The average of these sondes was a 32.3° inflow angle.

*c. Radius of influence*

Just as the intensity of a TC varies for each individual storm, the extent to which it has an effect on the surrounding area is also variable. The distance from the center of the storm where the mean tangential flow becomes anticyclonic is calculated using the NESDIS processed speeds and directions that were assigned to the three cases. Each observation location is defined by its distance away from the center of the storm,  $r$ , and its azimuth. The distance is found using the following equation:

$$r = [\bar{u}_v^2 + \bar{v}_v^2]^{1/2}. \quad (5)$$

The data is then placed into bins according to their radial distance from the center beginning at 0 km and continuing up to 550km, with 50 km worth of data in each bin. The wind vectors are then broken down into tangential and radial components relative to the center of the storm. The average of the tangential components of all observations in each bin is computed. If that value is negative, implying anticyclonic rotation, then the preceding bin is the upper limit of observations

considered for further analysis. Only the observations within an 8° box (4° North, 4° South, 4° East and 4° West) of the center are considered when performing an analysis in H\*Wind, therefore a radial distance of 550 km (approximately 5°) is sufficient for calculating the extent of the influence of the storm.

*d. Selection window*

In order to account for atmospheric conditions that might slightly affect constant inflow around the vortex, it is necessary to include surface wind ambiguities that may deviate from the assumed direction derived in the algorithm. To determine the optimum size of the window on either side of the ‘TC guess’ wind direction for which the observations would be retained, we will examine how the variance of the selected ambiguities within the radius of influence changes with the size of the window and the magnitude of the inflow used for the ‘TC guess’. The normalized total variance, combining the variance in the tangential wind component,  $V_t$ , and the variance in the radial wind component,  $V_r$  of the data can be expressed as:

$$V_{nT} = [(\sum V_t)^2 + (\sum V_r)^2]^{1/2} / n * 100 \quad (6)$$

with n representing the number of observation locations. By examining this value for the three cases, assuming that all four quadrants are experiencing the same inflow, it becomes evident that for inflows ranging from 25° to 35° there is a minimum in the variance when including only those wind directions approximately 30° on either side of a given inflow (FIGURE 1).

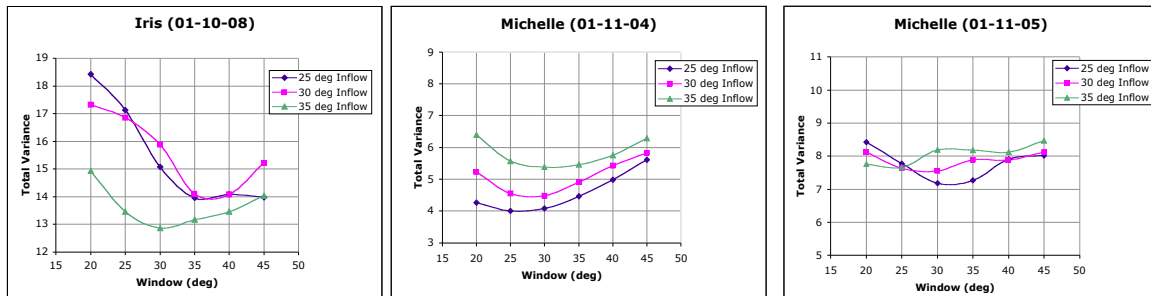


FIGURE 1. Total Normalized variance with respect to window size. Notice that each given inflow angle provides a minimum variance at  $25^{\circ}$ - $35^{\circ}$ , most occurring very close to  $30^{\circ}$ .

This range includes 79.5% of the dropsondes used in the study. Increasing the window size would result in more solutions that fit the criteria, however, the variance in the flow would also increase as well.

*e. Algorithm*

The following is the proposed dealiasing process for tropical cyclone QuikSCAT surface wind observations brought into H\*Wind. The default radius of influence is calculated by determining where the mean tangential flow around the TC turns anticyclonic using the NESDIS processed solutions. However, the user will have the option to change this value if it appears to be inconsistent with other observation platforms. Only the QuikSCAT observations within that radius are included in the algorithm to avoid applying an inflow to those that are not affected by the TC. For those observations whose distances from the center place them outside of the influence of the TC, the NESDIS values are retained. If the influence happens to extend farther out than 550 km ( $\sim 10^{\circ}$ ) then the algorithm is applied to all of the incoming data.

Each observation position is then converted to virtual latitude and longitude, and the azimuth is computed, as shown in FIGURE 2. The tangent angle, represented by the black arrow, is calculated by subtracting  $90^{\circ}$  from the azimuth. Each wind ambiguity is then subtracted from the tangent to obtain the inflow angle. Given the ‘TC guess’ wind flow direction of  $32.2^{\circ}$  inward from tangent, and a window of  $30^{\circ}$  on either side of that value, those observations which result in inflow from  $2.3^{\circ}$  to  $62.3^{\circ}$  around the given center location of the TC are preserved (FIGURE 2). The resulting observations are then available for the user to quality control.

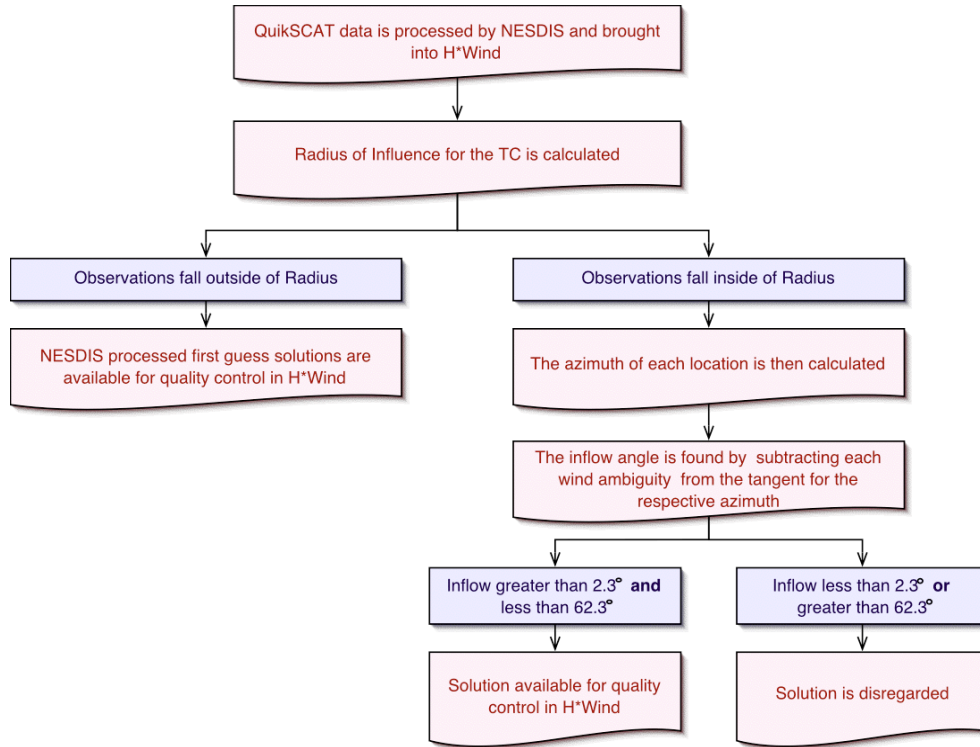


FIGURE 2. The algorithm.

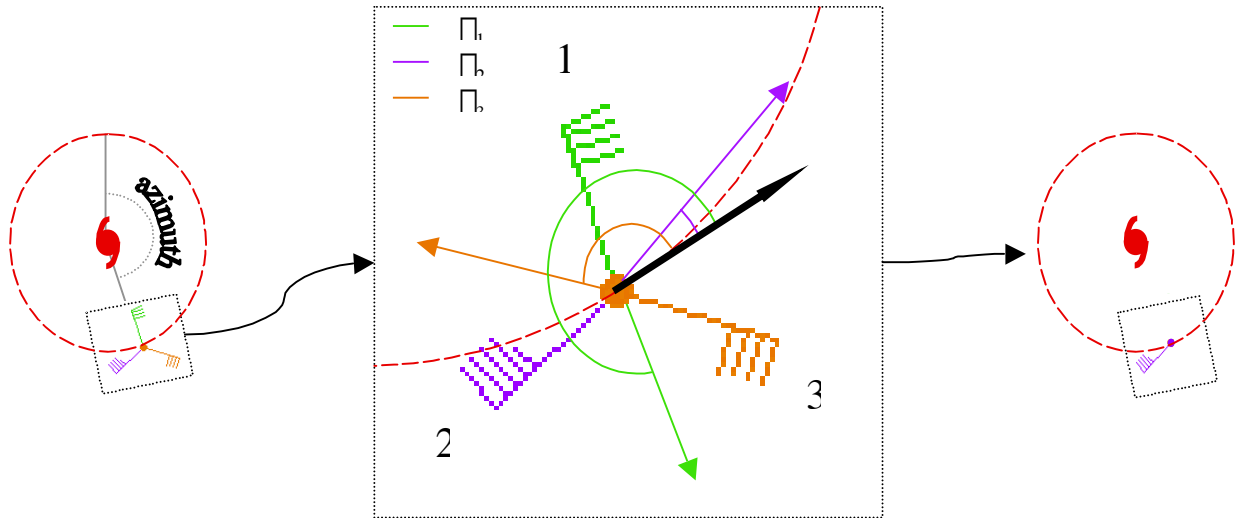


FIGURE 2. Here we have three wind ambiguities for a single location. Zooming in we can see that  $\theta_1 > 62.3^\circ$  and  $\theta_3 \gg 62.3^\circ$ .  $\theta_2$ , however, satisfies the algorithm's criteria that  $2.3^\circ > \theta > 62.3^\circ$  and the final schematic shows the resulting solution for that location.



### 3. RESULTS

#### *a. Hurricane Iris*

Hurricane Iris evolved from a tropical depression into a tropical storm in just 24 hours, with her circulation center on October 6 just south of Hispaniola in the Caribbean Sea. As the pressure continued to drop and the winds continued to intensify, Iris moved to the west with the outer bands extending over Honduras on 8 October. The QuikSCAT observations that were received in H\*Wind at 1127 UTC for Hurricane Iris on 8 October showed an easterly flow over the entire storm, and did not acknowledge any sign of a closed circulation at the surface (FIGURE 3A). At the same time, however, the satellite image clearly shows the developed hurricane in the area covered by the swath (FIGURE 3C). Although the satellite image displays the storm at 1800 UTC, the best track intensities and locations do not imply any major changes in the storm over those six hours. After applying the algorithm to the 1127 UTC pass, the vectors which passed through the algorithm, (FIGURE 3B), portray a more reasonable wind field at the surface, given the obvious low level circulation shown in the satellite image. The center of the storm, represented by the blue circles, is defined by interpolating between reconnaissance aircraft observed centers to the time of the QuikSCAT pass. Iris was a relatively small storm, with the influence only extending out about 150 km from the center, so the easterly winds are retained for the remainder of the swath.

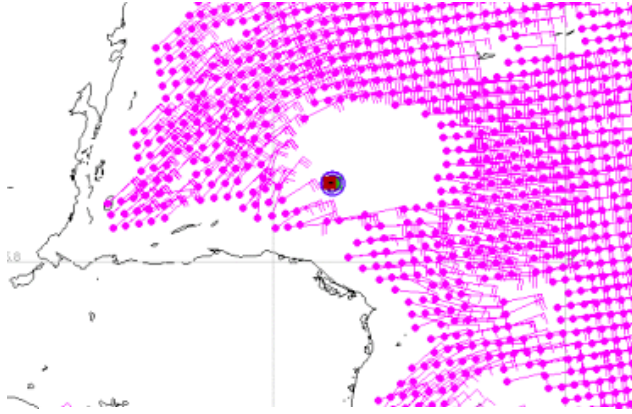


FIGURE 3A. QuikSCAT observations for Hurricane Iris sent in real-time to H\*Wind database (1127 UTC on October 8, 2001)

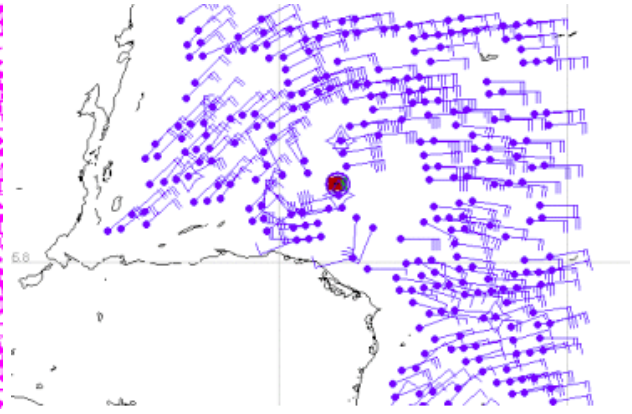


FIGURE 3B. Winds for the same time derived by the algorithm.

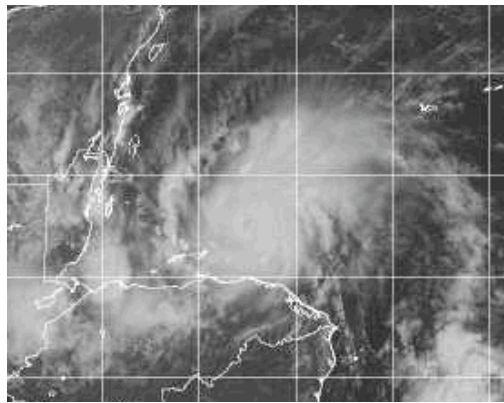


FIGURE 3C. Satellite image of Hurricane Iris (1800 UTC, October 8, 2001)

#### *b. Hurricane Michelle*

On 4 November, as Hurricane Michelle was approaching south-central Cuba, the satellite did not pass directly over the storm, giving poor coverage directly to the east. The NESDIS first guess solutions appear to have picked up a circulation, however they do not correspond with the location of the storm, represented by the blue circles in FIGURE 4, based on the aircraft vortex centers. The algorithm, with the circulation center at the time of the satellite pass, selects wind solutions that appear to be more accurate in that they show a cyclonic flow around the actual

center. Unfortunately, with the position of the storm relative to the pass, it can not be determined how both the first guess vectors and the algorithm vectors would have handled the other half of the storm.

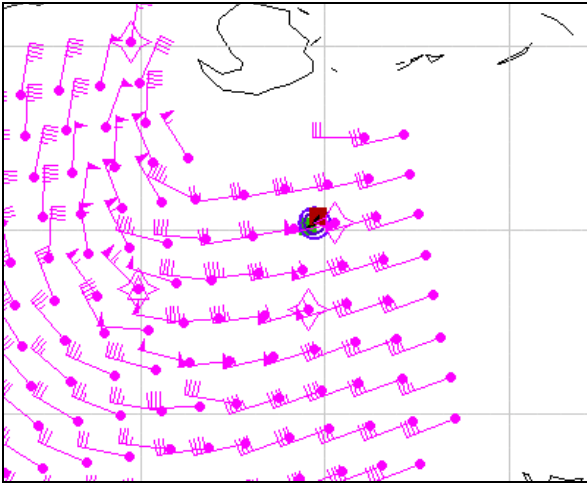


FIGURE 4A. 1142 UTC real-time QuikSCAT winds on 4 November for Hurricane Michelle

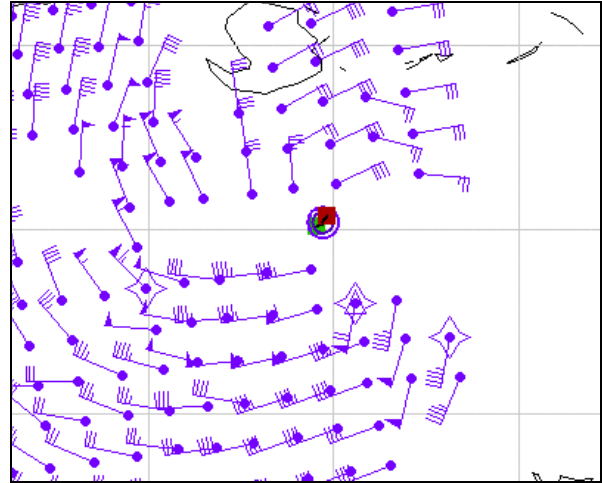


FIGURE 4B. Algorithm wind solutions.

By 5 November, 2001, Hurricane Michelle had moved off of the coast of Cuba onto the Grand Bahama Bank west of Andros Island, maintaining winds of 80 knots. Although the storm eye had dissipated and some of the bands were torn apart by the topography, there was still strong evidence of a large cyclonic rotation about the center. This becomes evident by displaying the winds measured by aircraft in the H\*Wind display (the red observations in FIGURE 5). By plotting both the QuikSCAT winds received in real-time (FIGURE 5A) and the observations processed by the algorithm (FIGURE 5B) over the aircraft winds, they can be compared to the aircraft platform, which is the primary source of high resolution wind information in regions experiencing gale force and hurricane force winds.

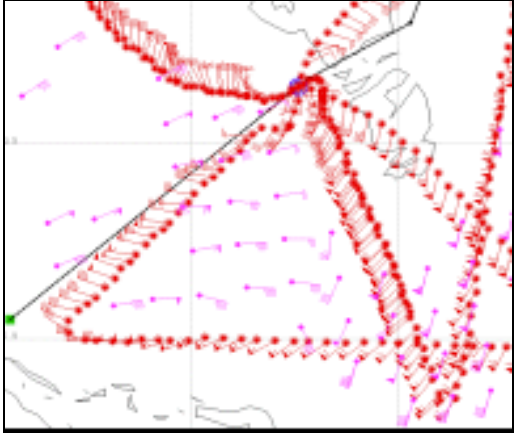


FIGURE 5A. 1118 UTC real-time QuikSCAT winds (purple) on November 5 for Hurricane Michelle compared with 1100 UTC-1300 UTC aircraft winds

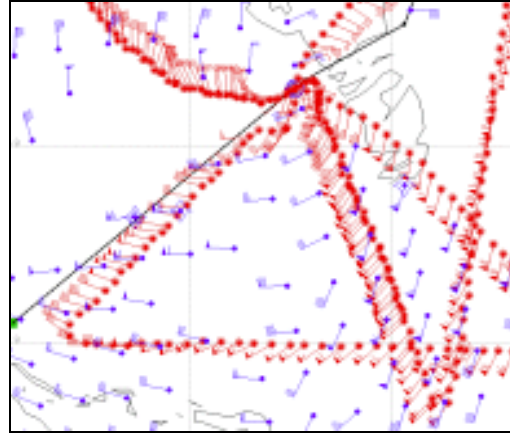


FIGURE 5B. Algorithm winds (blue) vs. aircraft winds (red)

Due to the relatively large size of Hurricane Michelle, the data representing the algorithm-processed winds consists entirely of wind directions chosen by the algorithm. Both the QuikSCAT and the algorithm observations do not seem to have a problem picking up the south-southwesterly flow in the southeast quadrant of the storm. For the real-time QuikSCAT data, there is, however, a significant difference between the wind directions in the southwest quadrant. The aircraft was experiencing the westerly flow typically associated with this particular area of a TC, while the QuikSCAT winds are showing an easterly flow - at some points appearing to have  $180^\circ$  of separation. The algorithm successfully filtered out those ambiguities that violated the inflow criteria and agreeably displays the westerly flow.

#### 4. SUMMARY and CONCLUSIONS

This method of dealiasing QuikSCAT wind ambiguities is simply used to better depict the QuikSCAT observed winds around a tropical cyclone for the purpose of performing a surface wind analysis. In cases where there is no clearly defined center of circulation, as with weak

tropical depressions and areas with no tropical development at all, the method will not apply. When these situations occur, H\*Wind will simply use the NESDIS first guess wind vectors. By implementing the algorithm into H\*Wind, the user will have an opportunity to choose whether or not the real-time processed QuikSCAT data is applicable to a given weather system, and adjust the observations accordingly. The surface wind analyses produced using the algorithm-derived winds will more accurately represent the situation at the surface for the time of the analysis, and thus provide enhanced guidance to the operational forecasters.

The results of this paper open the door to possible further research on dealiasing QuikSCAT wind ambiguities for a TC. An average inflow for all storm relative quadrants and distances within the influence of the storm was used to calculate the assumed flow. There may, in fact, be a correlation between the storm relative position of the observation location and the average inflow, which would provide a way to generalize storms and collectively analyze them. Storm size and intensity may also play a role in surface wind inflow; by grouping storms accordingly, it can be determined if that relationship exists. Also, the average inflow angle for a TC in this study was found to be  $32.2^\circ$ , however H\*Wind currently applies an inflow of only  $20^\circ$  when assigning headings to wind speed observations lacking direction around a TC. The  $20^\circ$  value is based on a subset of NOAA moored buoy and C-MAN stations in the vicinity of aircraft observations in Atlantic Hurricanes from 1979-1991 (Powell personal communication) I'm unsure how I should cite this). An expanded examination of storms since 1997 that have GPS dropsonde surface inflow angles available is warranted to determine whether  $20^\circ$  is too small of an angle for other platforms.

## 5. REFERENCES

- Hock, T.F., and J.L. Franklin, 1999: The NCAR GPS Dropwindsonde, *Bulletin of the American Meteorological Society*, 80, 407-420.
- Katsaros, K.B., E.B. Forde, P. Chang, and W.T. Liu, 2001: QuikSCAT's SeaWinds facilitates early identification of tropical depressions in 1999 hurricane season, *Geophysical Research Letters*, 28, 1043-1046.
- Lungu, T, ed., 2001: QuikSCAT Science Data Product User's Manual, 1-11.
- Otero, S., N. Morisseau-Leroy, N. Carrasco, and M.D. Powell, 2000: A distributed real-time hurricane wind analysis system, *Preprints, 24<sup>th</sup> Conference on Hurricanes and Tropical Meteorology*, 197-198.
- Powell, M.D., S.H. Houston, L.R. Amat, and N. Morisseau-Leroy, 1998: The HRD real-time hurricane wind analysis system. *Journal of Wind Engineering and Industrial Aerodynamics*, 77&78, 53-64.
- Ulaby, F.T., R.K. Moore, A.K. Fung, 1986: Microwave Remote Sensing, Vol. II, 841-842